

Utilization of *Gynura procumbens* leaf extract as a bioreductor for the synthesis of Ag/TiO₂ and Ag/ZnO and its application in multifunctional lotion

Tiur Elysabeth ^{1*}, Azzah Afifah N Cahyadi ¹, Siti Lailatul Jamila ¹, Euis Uswatun Hasanah ¹, Farid Wajdi ², Mohamad Jihan Shofa ², Athiek Sri Redjeki ³, Slamet ⁴

¹ Department of Chemical Engineering, Faculty of Engineering, Universitas Serang Raya, Serang, Indonesia

² Department of Industrial Engineering, Faculty of Engineering, Universitas Serang Raya, Serang, Indonesia

³ Department of Chemical Engineering, Faculty of Engineering, Universitas Muhammadiyah Jakarta, Central Jakarta, Indonesia

⁴ Department of Chemical Engineering, Faculty of Engineering, Universitas Indonesia, Depok, Indonesia

ABSTRACT

This study focused on the synthesis of sunscreen base materials utilizing photocatalytic substances, specifically TiO₂ and ZnO. The modification of TiO₂ and ZnO through the incorporation of Ag dopants aims to enhance their efficacy as sunscreens while also imparting antibacterial properties. The green synthesis employs natural materials, specifically the leaves of *Gynura procumbens*, which are rich in polyphenols for the reduction of Ag ions. The research methodology includes the extraction of *Gynura procumbens* leaves, the synthesis of Ag/TiO₂ and Ag/ZnO, characterization, and performance testing. Performance testing will evaluate the materials capabilities as sunscreens and antibacterial agents, as well as their effectiveness in lotion formulation. The results of FESEM EDX, XRD, and FTIR did not show any changes in the overall morphology and structure of TiO₂ and ZnO with the addition of Ag. However, the characterization results showed the presence of Ag in the structure of TiO₂ and ZnO. SPF and antibacterial tests were carried out to prove the sunscreen and antibacterial properties of Ag/TiO₂ and Ag/ZnO hybrid materials. The test results showed that there was an increase in the SPF value when Ag/TiO₂ and Ag/ZnO were added to the plain lotion from 0 to 1.23. The antibacterial test showed that with a higher concentration (15% Ag) Ag/TiO₂ can be antibacterial as evidenced by the emergence of an inhibition zone of 11.55 mm for *Staphylococcus aureus* during the incubation process for 24 h.

Keywords: Antibacterial agent, Bioreductor, Composite material, *Gynura procumbens*, Multifunctional lotion, Photocatalyst

OPEN ACCESS

Received: September 16, 2025


Revised: December 01, 2025

Accepted: December 22, 2025

Corresponding Author:

Tiur Elysabeth

tiurelysabeth@unsera.ac.id

 **Copyright:** The Author(s).

This is an open-access article distributed under the terms of the [Creative Commons Attribution License \(CC BY 4.0\)](https://creativecommons.org/licenses/by/4.0/), which permits unrestricted distribution provided the original author and source are cited.

Publisher:

[Chaoyang University of Technology](https://www.chaoyang.edu.cn/)

ISSN: 1727-2394 (Print)

ISSN: 1727-7841 (Online)

1. INTRODUCTION

The thinning of the ozone layer in the atmosphere has caused a rise in ultraviolet (UV) radiation. The UV radiation spectrum from solar rays is classified into three distinct wavelength ranges: UVA (320–400 nm), UVB (280–320 nm), and UVC (100–280 nm) (Parwaiz et al., 2019; Al-Attafi et al., 2023). The shorter wavelengths of UVC are fully absorbed by ozone, oxygen molecules, and atmospheric water vapor, resulting in the sunlight that reaches the earth being composed of approximately 95% UVA and the 5% UVB (Parwaiz et al., 2019; Tsunekawa et al., 2000). UVA can penetrate into the

subcutaneous tissue, while UVB can reach the outer epidermal layer (Truffault et al., 2012; Guan et al., 2021). This exposure to UVA and B radiation can lead to sunburn and DNA damage (Truffault et al., 2012; Guan et al., 2021), which may subsequently result in skin cancer.

The risk of skin damage due to UVA and UVB radiation can be mitigated through the use of cosmetics. In today's modern era, cosmetics have become an essential requirement, particularly for women. The application of cosmetics is not solely viewed from an aesthetic perspective but is also considered from a health standpoint. The inclusion of sunscreen in cosmetic products can significantly reduce the risk of skin cancer. Consequently, numerous researchers are focused on developing the ingredients found in cosmetics, especially sunscreens. However, organic materials commonly used in sunscreens may lead to skin irritation. In 2018, the Environmental Working Group (EWG) reported that two-thirds of sunscreens available in the United States contain chemicals that are harmful to the environment, with a majority being organic filters (Schneider and Lim, 2019). Research indicates that organic filters may have adverse hormonal effects on animals (Schlumpf et al., 2001), although no such effects have been documented in humans to date. This underscores the importance of conducting more comprehensive studies on the application of inorganic substances as foundational ingredients in sunscreen formulations. Beyond the risk of skin cancer associated with UV radiation, bacterial infections can also inflict harm on the skin's surface. The presence of polluted and humid air accelerates bacterial growth. *Staphylococcus* and *Streptococcus* are the predominant bacteria responsible for skin infections, often leading to the appearance of red rashes. Consequently, there is a pressing need for multifunctional cosmetics that not only shield the skin from UV rays but also possess antibacterial properties. These multifunctional products can be effectively utilized in multifunctional lotions.

Inorganic semiconductor materials, including TiO_2 and ZnO , have been confirmed to be safe for cosmetic use through their photocatalytic activities (Schneider and Lim, 2019; Syalsabilla et al., 2023; Sofaturrohman et al., 2024). These materials have wide energy band gaps that allow for effective UV light absorption, rendering them useful as sunscreen agents. However, there is a need for further investigation to modify these substances for incorporation into a multifunctional lotion that not only shields the skin from UV radiation but also protects against bacterial infections. The addition of silver (Ag) within the photocatalyst can provide antibacterial properties (Kubacka et al., 2013; Sahadewo et al., 2023). The primary concern, however, is the reduction of Ag ions, which often requires the use of dangerous, toxic, and expensive chemical reducing agents.

The application of plant extracts as bioreduction agents

can effectively resolve the issues related to nanoparticle synthesis. The exploration of green synthesis for Ag/TiO_2 composites using plant extracts has garnered significant attention and has been compared with the use of conventional chemical reducers. Various plant extracts, such as those from *Gynura procumbens* (Wahyuni et al., 2019), *Padina tetraströmatica* (Jegadeeswaran et al., 2015), Citrus citron (Liang et al., 2012), *Acacia nilotica* (Rao et al., 2019), *Nephelium lappaceum* (Kumar et al., 2016), *Euphorbia heterophylla* (Atarod et al., 2016), and *Origanum Majorana* (Bhardwaj and Singh, 2021), have been studied. The results suggest that the photocatalytic and biological efficacy of nanoparticles and nanocomposites can be enhanced through the implementation of green synthesis methods. *Gynura procumbens* is a perennial plant that is part of the Asteraceae family, known for its rich composition of triterpenoids, polyphenols, saponins, steroids, chlorogenic acid, caffeic acid, vanillic acid, coumaric acid, para-hydroxybenzoic acid, flavonoids, and essential oils (Priamsari et al., 2016). Flavonoids, which are a type of polyphenolic phytochemical, possess a stable phenolic structure. It is theorized that polyphenols can reduce Ag^+ ions to Ag^0 (Jain and Mehata, 2017; Alshehri and Malik, 2020).

Several researchers have carried out research on the synthesis of Ag/TiO_2 and Ag/ZnO for cosmetics but only focused on their function as sunscreen (Nicoara et al., 2020; Xin et al., 2023). Other researchers have synthesized Ag/TiO_2 and Ag/ZnO using chemicals as reducing agents (Li et al., 2017; Bartoszevska et al., 2023). A few researchers have used green synthesis to prepare Ag/TiO_2 and Ag/ZnO materials. Therefore, the research will focus on the advancement of TiO_2 and ZnO semiconductors that are doped with silver nanoparticles, employing the extract from *Gynura procumbens* leaves as a bioreductive agent for the reduction of silver ions. These materials will be integrated into a lotion formulation, functioning as both a sunscreen and an antibacterial agent with photocatalytic properties. The study aims to explore the modification of semiconductor materials TiO_2 and ZnO , utilizing them as sunscreen and antibacterial components in multifunctional lotions, thereby providing protection for the skin against UVA and UVB radiation and bacterial infections.

2. MATERIALS AND METHODS

2.1 Materials

The materials utilized in this research include *Gynura procumbens* leaves, ethanol, silver nitrate (AgNO_3), 65% nitric acid (HNO_3), titanium dioxide (TiO_2), zinc oxide (ZnO), distilled water, and a lotion with minimal ingredients. The equipment employed in this study consists of an analytical balance, maceration containers, aluminum foil, mortar and pestle, filter paper, labeling paper, erlenmeyer flasks, volumetric pipettes, dropper pipettes, pH meter, graduated cylinders, beakers, glass funnels, magnetic stirrer,

desiccator, distillation apparatus, water bath, sonicator, oven, and furnace.

2.2 The Extraction of *Gynura procumbens* Leaves

The sample preparation was conducted to obtain an extract from the *Gynura procumbens* leaves. The process commenced with washing and drying the leaves, followed by cutting them into smaller pieces and weighing 50 g, which were then placed into a maceration container. Subsequently, ethanol was added in a 1:1 ratio or until the leaves were fully submerged. The mixture was allowed to sit for 24 h to facilitate the extraction of compounds from the *Gynura procumbens* leaves. Afterward, the resulting macerate was filtered, and the soaking process with ethanol was repeated three times. The macerate obtained was then separated from the solvent, especially ethanol, using a rotary evaporator. The extract was then concentrated using a water bath.

2.3 Synthesis of Composite Materials

The process of synthesizing the composite material commences with the measurement of 2 g each of TiO_2 and ZnO , which are subsequently dissolved in 170 mL of deionized water. Following this, HNO_3 is gradually added until the pH reaches 3, and the mixture is subjected to sonication for a duration of 20 min. AgNO_3 is then introduced in concentrations of 1%, 2%, 3%, and 5% based on the weight of the photocatalyst, and the solution is stirred until it becomes homogeneous. The next step involves adding 30, 40, and 50 mL of extract from the *Gynura procumbens* leaves, which is stirred with a magnetic stirrer for 4 h until the solution exhibits a brown color, signifying the successful reduction of Ag ions by the leaf extract. After the stirring process is completed, the precipitate is washed twice with deionized water and dried in an oven at 90°C for 6 h. The final step involves calcining the material in a furnace at 250°C for 1 h, allowing it to cool to room temperature, after which it is ground and stored in a desiccator.

2.4 Characterization of Composite Materials

Characterization aims to evaluate the impact of *Gynura procumbens* leaves as a bioreductor on composite materials. The study will analyze changes in structure, morphology, properties, crystallography, and identification of functional groups. The crystal structure of the sample was examined using X-ray diffraction (XRD) with a SHIMADZU MAXima X XRD-7000 device, which was operated at 40 kV and 30 mA, utilizing $\text{Cu K}\alpha$ ($\lambda = 0.15406$ nm) as the source of the beam. The morphological assessment of the sample was achieved by analyzing the samples with a Field Emission Scanning Electron Microscope (FESEM, FEI Inspect F50). The sample's composition was evaluated through an Energy Dispersive X-ray analyzer (EDX, Oxford XMAX 50 detector, High Wycombe, UK). The analysis of the chemical's structure was performed utilizing

a Fourier Transform Infrared Spectrometer (FTIR, Thermo Scientific, Nicolet IS5).

2.5 Development of a Multifunctional Lotion

In this phase, lotions found in the market are designed with a minimal ingredient profile, incorporating Ag/TiO_2 and Ag/ZnO to enhance their multifunctional properties. The formulation process involves mixing the lotion with 1% Ag/TiO_2 and Ag/ZnO , followed by sonication to ensure a uniform consistency.

2.6 Analysis of Multifunctional Lotion Properties

The multifunctional lotion developed through the engineering process was then evaluated for its efficacy as a sunscreen and antibacterial agent. The assessment involved disinfection of *Staphylococcus aureus* and *Staphylococcus epidermidis* bacteria. This evaluation was carried out using the disk diffusion antibiotic sensitivity testing method. In addition, the multifunctional lotion underwent in vitro testing to determine its Sun Protection Factor (SPF). To evaluate the efficacy of sunscreen, the SPF value is determined in vitro using a UV-Vis spectrophotometer. The lotion, enhanced with Ag/TiO_2 and Ag/ZnO components, is diluted and analyzed with the spectrophotometer over a wavelength range of 290–320 nm, measured at 5 nm intervals, while 70% ethanol is employed as the blank solution.

3. RESULTS AND DISCUSSION

3.1 Characterization of Composite Materials

The color change of AgNO_3 solution to brown indicates that the reduction process using natural reducing agent *Gynura procumbens* leaf extract has been successful as shown in Fig. 1. The solution is combined with TiO_2 and ZnO to form hybrid compounds Ag/TiO_2 and Ag/ZnO with each composition that has been determined.

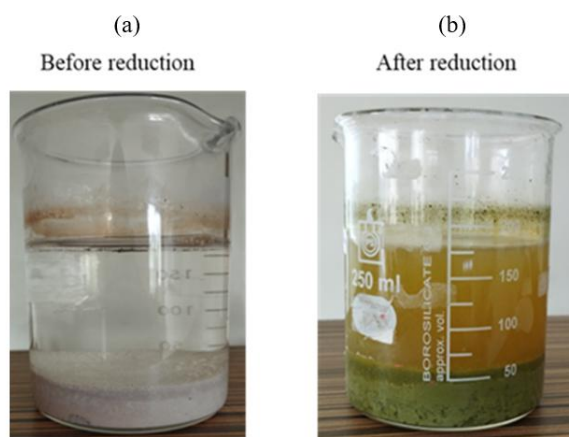


Fig. 1. The difference in color of solution before and after reduction process

Table 1. The naming of samples in the research findings

Sample	Sample name	Information
1	TiO ₂ / 1% AgNO ₃ ES	Combination of TiO ₂ and reduced 1% AgNO ₃ with 40 mL of fresh leaf extract
2	TiO ₂ / 1% AgNO ₃ EK	Combination of TiO ₂ and reduced 1% AgNO ₃ with 40 mL of commercial leaf extract
3	TiO ₂ / 2% AgNO ₃ EK	Combination of TiO ₂ and reduced 2% AgNO ₃ with 40 mL of commercial leaf extract
4	TiO ₂ / 3% AgNO ₃ EK	Combination of TiO ₂ and reduced 3% AgNO ₃ with 40 mL of extract commercial leaf chocolate bottle
5	TiO ₂ / 5% AgNO ₃ EK	Combination of TiO ₂ and reduced 5% AgNO ₃ with 40 mL of commercial leaf extract
6	ZnO / 5% AgNO ₃ EK	Combination of ZnO and reduced 5% AgNO ₃ with 40 mL of commercial leaf extract

The objective of characterization is to investigate the effect of *Gynura procumbens* leaves as a bioreductor on composite materials. Changes in structure, morphology, properties, crystallography, and light absorption will be analyzed using FESEM EDX, XRD, and FTIR techniques. Sample naming is shown in Table 1.

The arrangement of nanotubes on the titanium substrate is influenced by the competitive reactions of oxidation layer formation and chemical dissolution (Liang and Li, 2009). FESEM characterization was performed to analyze the surface morphology of the synthesized Ag/TiO₂ and Ag/ZnO as well as to determine the material composition and the distribution of the components within Ag/TiO₂ and Ag/ZnO, as illustrated in Fig. 2 and Table 2.

The morphology of Ag/TiO₂, as depicted in Fig. 2, illustrates the reduction achieved by fresh *Gynura procumbens* leaf extract and commercial extract. Samples reduced with fresh *Gynura procumbens* leaf extract showed uneven particle size and the presence of agglomerates, especially in the Ag/TiO₂ sample treated with fresh leaves. These agglomerates are likely composed of Ag particles attached to the TiO₂ surface, indicating that the *Gynura procumbens* leaf extract effectively reduced Ag⁺ to Ag⁰. Similar results for Ag/ZnO are shown in Fig. 2(f). The presence of silver in the composite material is further confirmed by the EDX results presented in Table 2. The table reveals that sample 1, extracted using fresh leaves, contains a higher concentration of Ag compared to the commercially extracted one. Samples 2–5 illustrate the variation of silver content based on the percentage of silver nitrate used during synthesis. The concentrations of AgNO₃ used were 1%, 2%, 3%, and 5%. EDX results showed a correlation between the amount of AgNO₃ precursor and the amount of Ag present in the composite material. Increasing the amount of AgNO₃ resulted in higher detection of Ag on the TiO₂ surface. However, in sample number 5, where 5% AgNO₃ was used, the percentage of Ag on the TiO₂ surface was lower compared to samples 3 and 4. This phenomenon is non-uniform deposition on the TiO₂ surface and Ag particles do not adhere well to TiO₂. Different results were

shown by sample 6. The Ag content in this material is much higher than Ag/TiO₂. The deposition of Ag on ZnO looks more even, this is because Ag adhered more to ZnO. Research conducted by Riya et al (2024) also obtained similar results (Zhang et al., 2014; Shah et al., 2024). XRD characterization is employed to ascertain the crystalline structure of a material. The type of material can be identified by comparing the XRD characterization results with the diffraction peaks found in a catalog. In this characterization, the synthesized Ag/TiO₂ catalyst will be compared to TiO₂ P25. The results of the XRD characterization are presented in Fig. 3.

Based on the analysis presented in Fig. 3, it can be concluded that the primary crystals identified are anatase and rutile forms of TiO₂. In contrast, the silver peaks are only faintly observed in the XRD characterization results, with silver detected at 2θ = 64° and silver oxide at 2θ = 32° (Gauri et al., 2016). The presence of AgO crystals is attributed to the interaction of the synthesized Ag/TiO₂ sample with air following the preparation process, leading to the oxidation of Ag⁰ into AgO (Tseng and Chen, 2019).

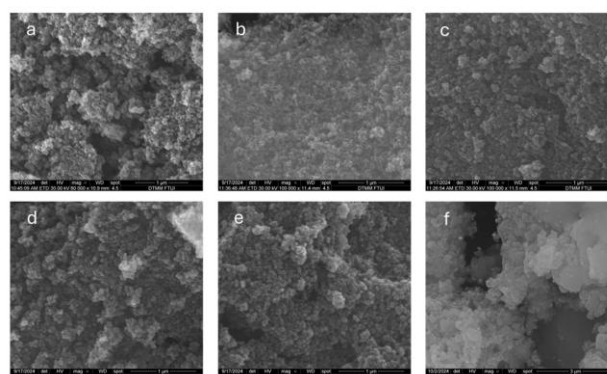


Fig. 2. FESEM images: (a) sample 1, (b) sample 2, (c) sample 3, (d) sample 4, (e) sample 5, and (f) sample 6

The results of XRD analysis of Ag/ZnO are shown in Fig. 4. From the X-ray diffraction pattern of the XRD analysis results in Fig. 4 a sharp and narrow curve line can be seen.

This indicates that the compound formed is in a crystalline phase. The presence of Ag in the ZnO structure is shown in peaks $2\theta = 38^\circ, 44^\circ,$ and 77° .

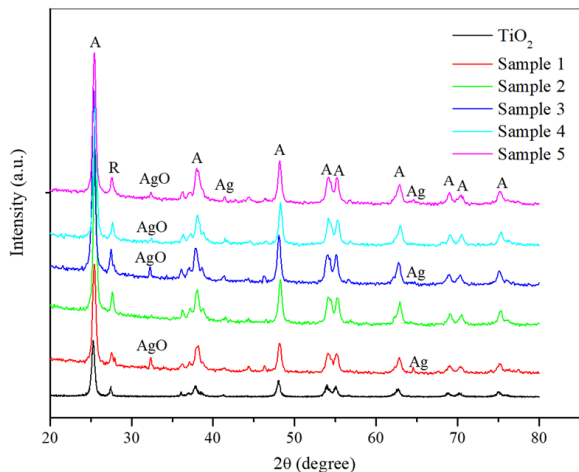


Fig. 3. XRD patterns of TiO₂ and Ag/TiO₂

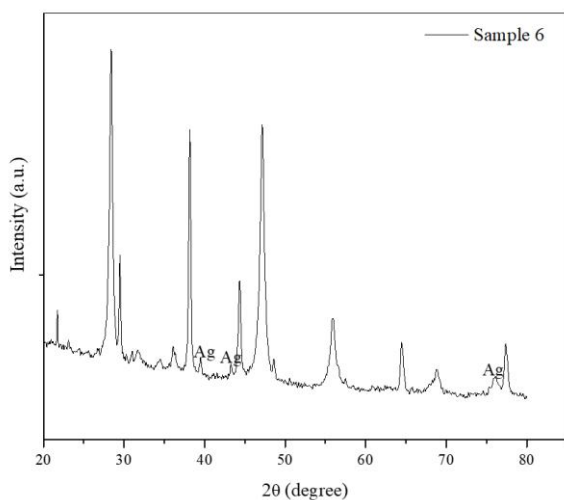


Fig. 4. XRD pattern of Ag/ZnO

Anatase crystals are recognized as the most active in photocatalytic processes. An increase in the quantity of anatase crystals within the catalyst correlates positively with the photocatalytic performance, although the presence of rutile crystals also holds significant importance. This indicates that the catalyst is not amorphous and is free from impurities, thereby demonstrating a more crystalline catalyst structure. Crystalline regions display a well-organized structure with tightly packed molecules, in contrast, amorphous regions are defined by their absence of structural order and a more loosely arranged configuration (Jose et al., 2024). The composition ratio between anatase and rutile is also crucial, with a higher proportion of anatase being preferable in the catalyst, accompanied by a minimal amount of rutile crystals to achieve optimal effectiveness in photocatalysis (Slamet et al., 2005). Functional groups

formed in the Ag/TiO₂ are identified by several peaks in the FTIR transmission spectrum, measured in range of 3500 – 400 cm⁻¹, as illustrated in Fig. 5(a). The peak observed around 1600 cm⁻¹ corresponds to the hydroxyl group (-OH) (Feng et al., 2021), while the peaks between 400 and 800 cm⁻¹ are associated with the Ti-O-Ti bonds present in titanium nanoparticles (Ansari et al., 2012). According to the literature, the FTIR spectrum near 1050 cm⁻¹ is identified as the Ag nanoparticles (Jayapriya and Arulmozhi, 2021). The FTIR characterization spectrum illustrated in Fig. 5(b) reveals multiple peaks within the wavenumber range of 400 to 3,500 cm⁻¹. Notably, peaks at approximately 874 cm⁻¹ are indicative of tetrahedral Zn bonds. Additionally, a peak near 3,367 cm⁻¹ corresponds to stretching vibrations of the hydroxyl bond O-H. A distinct peak around 1,558 cm⁻¹ is linked to H-O-H bending vibrations, reflecting a minor presence of H₂O within the ZnO nanocrystals (Muthukumaran and Gopalakrishnan, 2012). Furthermore, the FTIR spectrum displays a peak around 1050 cm⁻¹, which signifies the existence of Ag-O nanoparticles (Jayapriya and Arulmozhi, 2021).

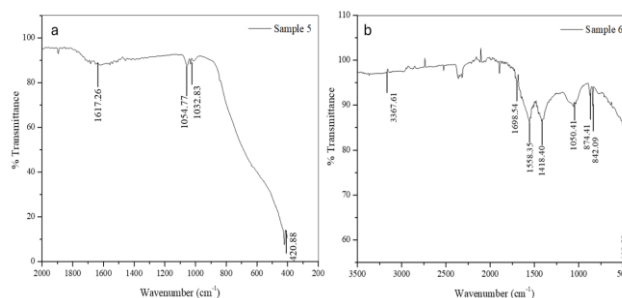


Fig. 5. FTIR spectrum of (a) Ag/TiO₂ and (b) Ag/ZnO

3.2 SPF and Antibacterial Test

A sunscreen is a product that comprises ingredients that can absorb, scatter, or reflect ultraviolet rays from the sun, which interact with the skin, thus providing a protective barrier for the skin's functions and structure against the harmful effects of solar exposure. SPF quantifies the degree of protection afforded to the skin, indicating how many times longer a person can be exposed to sunlight without developing erythema; consequently, a higher SPF rating signifies superior protective performance. This study establishes SPF value determination as a critical parameter for evaluating the potential of sunscreen. SPF quantifies the effectiveness of various sunscreen formulations. It conducted in vitro and assessed via a UV-VIS spectrophotometer.

SPF was assessed in accordance with the methodology proposed by researchers (Mansur et al., 1986; Sharma et al., 2020). The absorbance of the samples was evaluated within the UV-B wavelength range of 290 to 320 nm, with 5 nm increments, and three determinations were conducted at each specified wavelength. The SPF was computed by applying the Mansur equation.

$$SPF = CF \times EE(\lambda) \times I(\lambda) \times Abs(\lambda) \quad (1)$$

where:

- CF = correction factor (10)
- EE = erythemogenic effect of radiation with wavelength
- I = solar intensity spectrum
- Abs (λ) = spectrophotometric absorbance values at wavelength

Table 3 shows the results of SPF calculations for several samples. The table shows that there is an increase in the SPF value before and after the lotion is added with Ag/TiO₂ and Ag/ZnO materials. This shows that the modification process has been successful. However, the SPF value has not shown a high number according to World Health Organization (WHO) standards. This is because the composition of Ag/TiO₂ and Ag/ZnO is only 1% of the total lotion weight. Therefore, further research is needed for the best composition to obtain the optimal SPF value.

Table 3. Sun Protective Factor (SPF) values

Sample	SPF values
Plain lotion	0
Sample 2	1.23
Sample 3	0.7
Sample 4	0.47
Sample 5	0.28
Sample 6	1.19

The integration of Ag into TiO₂ improves UV absorption and enhances light-material interaction. However, a higher concentration of Ag concurrently increases photocatalytic activity, causes particle agglomeration, and induces spectral red-shifting effects. These occurrences diminish the uniformity and efficiency of UV scattering within the sunscreen film, resulting in heightened UV transmission and consequently a reduced SPF. Thus, beyond a certain optimal concentration, Ag functions more as a destabilizing agent than as a protective enhancer in TiO₂-based sunscreen formulations.

Antibacterial test was conducted using the Kirby-Bauer disk diffusion method. The bacteria used were *Staphylococcus aureus* and *Staphylococcus epidermidis*. In the assessment of antibacterial activity, 6 mm paper discs with a capacity to absorb 50 μ L per disc were utilized. Each disc was treated with samples at a specified concentration of 250 μ g/50 μ L, applied using a micropipette. Nutrient Agar (NA), which had been autoclaved at 121°C for 15 min, was subsequently cooled to 40°C. Following this, the cooled NA was poured into a petri dish, and 100 μ L of bacteria cultured in a test tube was pipetted into the NA, allowing it

to solidify. Each petri dish was appropriately labeled with a corresponding sample number. The paper discs, which had been treated with the test sample derived from *Theonella swinhoei* sponge, were carefully placed in the petri dish using tweezers and incubated for a duration of 24 h (Ortez, 2005).

The results of the antibacterial test are shown in Table 4. The test results show that the composition of Ag and TiO₂ in samples 1–5 cannot be antibacterial. It is because the composition of Ag is very small and the test was carried out in conditions without UV light. The second test was carried out by increasing the levels of Ag in TiO₂ and ZnO to 15% and was still carried out without UV light. The results are shown in Table 5, where Ag/TiO₂ shows antibacterial properties with an inhibition zone of 11.55 mm for *Staphylococcus aureus*. Despite the 15% Ag/TiO₂ sample demonstrating a bacterial inhibition of 11%, this figure was significantly less than the control's 40%. This suggests that incorporating 15% Ag/TiO₂ did not enhance antibacterial effectiveness and should not be regarded as a viable antibacterial treatment within the parameters of the experiment. Consequently, its inhibitory impact may be deemed minimal and necessitates additional optimization.

The incubation process of *Staphylococcus aureus* bacteria is shown in Fig. 6. The research conducted by Yue Lin et al. highlighted the antibacterial activity of Ag/TiO₂ core/shell nanoparticles against *Escherichia coli* without the application of UV light. They noted a pronounced inhibition zone around the hybrid nanoparticles, contrasting with the absence of an inhibition zone in the case of TiO₂ nanoparticles (Lin et al., 2011; Nguyen et al., 2019). This observation underscores the significant role that silver nanoparticles play in imparting antibacterial characteristics.

While Ag/ZnO has not shown antibacterial properties. This may be because the test was carried out in conditions without light and the Ag content in ZnO is mostly not Ag⁰ but AgO. Of course, this opinion needs to be tested again with more comprehensive research.

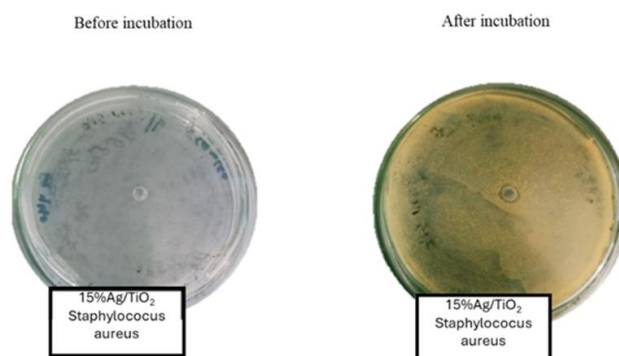


Fig. 6. Image of antibacterial test against *Staphylococcus aureus* for 15% Ag/TiO₂ without light irradiation

Table 4. Antibacterial test results 1

Sample	Microorganism strains	ZOI	Unit
Sample 1	<i>Staphylococcus aureus</i>	0	mm
	<i>Staphylococcus epidermidis</i>	0	
Sample 2	<i>Staphylococcus aureus</i>	0	
	<i>Staphylococcus epidermidis</i>	0	
Sample 3	<i>Staphylococcus aureus</i>	0	
	<i>Staphylococcus epidermidis</i>	0	
Sample 4	<i>Staphylococcus aureus</i>	0	
	<i>Staphylococcus epidermidis</i>	0	
Sample 5	<i>Staphylococcus aureus</i>	0	
	<i>Staphylococcus epidermidis</i>	0	
Sample 6	<i>Staphylococcus aureus</i>	0	
	<i>Staphylococcus epidermidis</i>	0	
Control	<i>Staphylococcus aureus</i>	36	
	<i>Staphylococcus epidermidis</i>	34.3	

Table 5. Antibacterial test results 2

Sample	Microorganism strains	ZOI	Unit
15% Ag/TiO ₂	<i>Staphylococcus aureus</i>	11.55	mm
	<i>Staphylococcus epidermidis</i>	0	
15% Ag/ZnO	<i>Staphylococcus aureus</i>	0	
	<i>Staphylococcus epidermidis</i>	0	
Control	<i>Staphylococcus aureus</i>	40.5	
	<i>Staphylococcus epidermidis</i>	40.8	

4. CONCLUSION

This research successfully created a multifunctional lotion utilizing a green synthesis method, employing *Gynura procumbens* leaf extract as a natural reducing agent to convert Ag⁺ to Ag⁰, as evidenced by the distinct color change of the solution. The effective formation of Ag/TiO₂ and Ag/ZnO hybrid materials was validated through FESEM-EDX, XRD, and FTIR analyses, which indicated that the incorporation of Ag did not significantly modify the morphology or crystal structure of TiO₂ and ZnO.

The primary role of sunscreen is to shield the skin from UV radiation and mitigate the risk of skin damage. The incorporation of Ag/TiO₂ and Ag/ZnO elevated the SPF value of the lotion from 0 to a peak of 1.23, however, this figure remains below the minimum recommended SPF of 2 as per WHO guidelines, suggesting that the formulation is not yet effective as a sunscreen. Likewise, the antibacterial assessment revealed that the lotion containing 15% Ag/TiO₂ yielded a bacterial inhibition value of 11%, which is significantly lower than the control (40%), indicating limited antibacterial efficacy.

Furthermore, sunscreen formulations must guarantee

safety for prolonged use, and the concentration of silver-based additives should stay within non-toxic thresholds. Consequently, while the developed lotion exhibits potential multifunctionality, its current performance is still inadequate. Additional optimization of Ag/TiO₂ and Ag/ZnO concentrations, enhanced dispersion, quantitative silver analysis, and thorough safety assessments are necessary to improve both efficacy and skin compatibility.

DECLARATION OF COMPETING INTEREST

We have no known competing financial interests or personal relationships that could have appeared to influence the work reported in this paper.

ACKNOWLEDGMENT

This project has received financial support from the Penelitian Fundamental Regular (PFR) Grant, overseen by the Directorate of Research, Technology, and Community Service under the Directorate General of Higher Education, Research, and Technology. The grant was issued by the Ministries of Education, Culture, Research, and Technology, and it is associated with the following contract

numbers 038/SP2H/RT-MONO/LL4/2024 and 009/DRTPM.PFR/UNSER/VI/2024.

REFERENCES

- Al-Attafi, K., Al-Keisy, A., Alsherbiny, M.A., Kim, J.H. 2023. Zn₂SnO₄ ternary metal oxide for ultraviolet radiation filter application: a comparative study with TiO₂ and ZnO. *Science and Technology of Advanced Materials*, 24, 2277678.
- Alshehri, A.A., Malik, M.A. 2020. Phytomediated photo-induced green synthesis of silver nanoparticles using *Matricaria chamomilla* L. and its catalytic activity against rhodamine B. *Biomolecules*, 10, 1604.
- Ansari, S.G., Bhayana, L., Umar, A., Al-Hajry, A., Al-Deyab, S.S., Ansari, Z.A. 2012. Understanding the effect of flower extracts on the photoconducting properties of nanostructured TiO₂. *Journal of Nanoscience and Nanotechnology*, 12, 7860–7868.
- Atarod, M., Nasrollahzadeh, M., Sajadi, S.M. 2016. Euphorbia heterophylla leaf extract mediated green synthesis of Ag/TiO₂ nanocomposite and investigation of its excellent catalytic activity for reduction of variety of dyes in water. *Journal of Colloid and Interface Science*, 462, 272–279.
- Bartoszewska, M., Adamska, E., Kowalska, A., Grobelna, B. 2023. Novelty cosmetic filters based on nanomaterials composed of titanium dioxide nanoparticles. *Molecules*, 28, 645.
- Bhardwaj, D., Singh, R. 2021. Green biomimetic synthesis of Ag–TiO₂ nanocomposite using *Origanum majorana* leaf extract under sonication and their biological activities. *Bioresources and Bioprocessing*, 8, 1–2.
- Feng, J., Zhang, X., Zhang, G., Li, J., Song, W., Xu, Z. 2021. Improved photocatalytic conversion of high-concentration ammonia in water by low-cost Cu/TiO₂ and its mechanism study. *Chemosphere*, 274, 129689.
- Gauri, B., Vidya, K., Sharada, D., Shobha, W. 2016. Synthesis and characterization of Ag/AgO nanoparticles as alcohol sensor. *Journal of Chemical Environment*, 20, 1–5.
- Guan, L.L., Lim, H.W., Mohammad, T.F. 2021. Sunscreens and photoaging: a review of current literature. *American Journal of Clinical Dermatology*, 22, 819–828.
- Jain, S., Mehata, M.S. 2017. Medicinal plant leaf extract and pure flavonoid mediated green synthesis of silver nanoparticles and their enhanced antibacterial property. *Scientific Reports*, 7, 15867.
- Jayapriya, M., Arulmozhi, M. 2021. Beta vulgaris peel extract mediated synthesis of Ag/TiO₂ nanocomposite: characterization, evaluation of antibacterial and catalytic degradation of textile dyes-an electron relay effect. *Inorganic Chemistry Communications*, 128, 108529.
- Jegadeeswaran, P., Periakaruppan, R., Vanathi, P., Rajeshwari, S., Rajendran, V. 2015. A novel green technology: synthesis and characterization of Ag/TiO₂ nanocomposites using *Padina tetrastrum* (seaweed) extract. *Materials Letters*, 166.
- Jose, D., Vasudevan, S., Venkatachalam, P., Maity, S.K., Septevani, A.A., Gupta, M., Tantayotai, P., El Bari, H., Sriaryanun, M. 2024. Effective deep eutectic solvent pretreatment in one-pot lignocellulose biorefinery for ethanol production. *Industrial Crops and Products*, 222, 119626.
- Kubacka, A., Munoz-Batista, M.J., Ferrer, M., Fernández-García, M. 2013. UV and visible light optimization of anatase TiO₂ antimicrobial properties: surface deposition of metal and oxide (Cu, Zn, Ag) species. *Applied Catalysis B: Environmental*, 140, 680–690.
- Kumar, B., Smita, K., Angulo, Y., Cumbal, L. 2016. Valorization of rambutan peel for the synthesis of silver-doped titanium dioxide (Ag/TiO₂) nanoparticles. *Green Processing and Synthesis*, 5, 371–377.
- Li, S., Zhu, T., Huang, J., Guo, Q., Chen, G., Lai, Y. 2017. Durable antibacterial and UV-protective Ag/TiO₂@ fabrics for sustainable biomedical application. *International Journal of Nanomedicine*, 12, 2593–2606.
- Liang, H.-c., Li, X.-z. 2009. Effects of structure of anodic TiO₂ nanotube arrays on photocatalytic activity for the degradation of 2,3-dichlorophenol in aqueous solution. *Journal of Hazardous Materials*, 162, 1415–1422.
- Liang, W., Church, T.L., Harris, A.T. 2012. Biogenic synthesis of photocatalytically active Ag/TiO₂ and Au/TiO₂ composites. *Green chemistry*, 14, 968–975.
- Lin, Y., Qiqiang, W., Xiaoming, Z., Zhouping, W., Wenshui, X., Yuming, D. 2011. Synthesis of Ag/TiO₂ core/shell nanoparticles with antibacterial properties. *Bulletin of the Korean Chemical Society*, 32, 2607–2610.
- Mansur, J.d.S., Breder, M.N.R., Mansur, M.C.d.A., Azulay, R.D. 1986. Determinação do fator de proteção solar por espectrofotometria. *An. Bras. Dermatol*, 12–124.
- Muthukumar, S., Gopalakrishnan, R. 2012. Structural, FTIR and photoluminescence studies of Cu doped ZnO nanopowders by co-precipitation method. *Optical Materials*, 34, 1946–1953.
- Nguyen, V.T., Vu, T.V., Nguyen, T.H., Nguyen, T.A., Nguyen, T.V., Nguyen-Tri, P. 2019. Effect of silver decoration and light irradiation on the antibacterial activity of TiO₂ and ZnO nanoparticles. *Journal of Composites Science*, 3, 61.
- Nicoara, A.I., Ene, V.L., Voicu, B.B., Bucur, M.A., Neacsu, I.A., Vasile, B.S., Iordache, F. 2020. Biocompatible Ag/Fe-Enhanced TiO₂ Nanoparticles as an Effective Compound in Sunscreens. *Nanomaterials*, 10, 570.
- Ortez, J. 2005. Disk diffusion testing in manual of antimicrobial susceptibility testing. Marie B. Coyle.
- Parwaiz, S., Khan, M.M., Pradhan, D. 2019. CeO₂-based nanocomposites: an advanced alternative to TiO₂ and ZnO in sunscreens. *Materials Express*, 9, 185–202.
- Priamsari, M.R., Susanti, M.M., Atmaja, A.H. 2016. Pengaruh metode pengeringan terhadap kualitas ekstrak

- dan kadar flavonoid total ekstrak etanolik daun sambung nyawa (*Gynura procumbens* (Lour.) Merr.). *Jurnal Farmasi (Journal of Pharmacy)*, 5, 29–33.
- Rao, T.N., Babji, P., Ahmad, N., Khan, R.A., Hassan, I., Shahzad, S.A., Husain, F.M. 2019. Green synthesis and structural classification of *Acacia nilotica* mediated-silver doped titanium oxide (Ag/TiO₂) spherical nanoparticles: Assessment of its antimicrobial and anticancer activity. *Saudi Journal of Biological Sciences*, 26, 1385–1391.
- Sahadewo, A.H., Elysabeth, T., Slamet. 2023. Utilization of *Uncaria gambir* Roxb leaf extract as a reducing agent in the green synthesis of Ag/TiO₂ composites and its application for multifunctional towels. *Journal of Textile Research*, 93, 2849–2858.
- Schlumpf, M., Cotton, B., Conscience, M., Haller, V., Steinmann, B., Lichtensteiger, W. 2001. In vitro and in vivo estrogenicity of UV screens. *Environmental health perspective*, 109, 239–244.
- Schneider, S.L., Lim, H. W. 2019. A review of inorganic UV filters zinc oxide and titanium dioxide. *Photodermatology, photoimmunology and photomedicine*, 35, 442–446.
- Shah, R., Kumar, R.N., Ji, N.K., Goswami, N. 2024. An assessment of the antibacterial activity of Ag-Doped TiO₂ and Ag-Doped ZnO Nanoparticles. *Environment and Ecology*, 42, 1375–1381.
- Sharma, T., Tyagi, V., Bansal, M. 2020. Determination of sun protection factor of vegetable and fruit extracts using UV–Visible spectroscopy: A green approach. *Sustainable Chemistry and Pharmacy*, 18, 100347.
- Slamet, Nasution, HW., Purnama, E., Kosela, S., Gunlazuardi, J. 2005. Photocatalytic reduction of CO₂ on copper-doped Titania catalysts prepared by improved-impregnation method. *Catalysis Communications*, 6, 313–319.
- Sofaturrohan, F., Rifka, L., Syalsabilla, M., Syuriyani, M., Raisa, N., Jonuarti, R., Hidayat, R. 2024. Analysis Titanium Dioxide and Zinc Oxide in physical sunscreen commercial with protection value 35 SPF. *Pillar of Physics*, 17, 64–73.
- Syalsabilla, M., Sofaturahman, F., Syuriyani, M., Septiana, L.R., Aryani, N.R., Jonuarti, R., Hidayat, R. 2023. The effect of compositional optical analysis of ZnO/TiO₂ composites in a sunscreen product. *Pillar of Physics*, 16, 52–78.
- Truffault, L., Winton, B., Choquenot, B., Andreatza, C., Simmonard, C., Devers, T., Konstantinov, K., Couteau, C., Coiffard, L.J. 2012. Cerium oxide based particles as possible alternative to ZnO in sunscreens: effect of the synthesis method on the photoprotection results. *Materials Letters*, 68, 357–360.
- Tseng, H.-C., Chen, Y.-W. 2019. Facile synthesis of Ag/TiO₂ by photoreduction method and its degradation activity of methylene blue under UV and visible light irradiation. *Modern Research in Catalysis*, 9, 1–19.
- Tsunekawa, S., Fukuda, T., Kasuya, A. 2000. Blue shift in ultraviolet absorption spectra of monodisperse CeO_{2-x} nanoparticles. *Journal of Applied Physics*, 87, 1318–1321.
- Wahyuni, S., Syukri, S., Arief, S. 2019. Green synthesis of Ag/TiO₂ Nanocomposite Assisted by Gambier Leaf (*Uncaria gambir* Roxb) Extract. *Textile Research Journal*, 22, 6.
- Xin, J., Wang, J., Yao, Y., Wang, S., Zhang, Z., Yao, C. 2023. Improved simulated-daylight photodynamic therapy and possible mechanism of ag-modified TiO₂ on Melanoma. *International Journal of Molecular Sciences*, 24, 7061.
- Zhang, Q., Li, F., Chang, X., He, D. 2014. Comparison of Nickel Foam/Ag-Supported ZnO, TiO₂, and WO₃ for Toluene Photodegradation. *Materials and Manufacturing Processes*, 29, 789–794.